

# Symbolic Analysis of Switching Systems: Application to Bifurcation Analysis of DC/DC Switching Converters

Dong Dai, *Member, IEEE*, Chi K. Tse, *Senior Member, IEEE*, and Xikui Ma

**Abstract**—A symbolic method is proposed in this paper for analyzing the bifurcation behavior of switching nonsmooth systems. The proposed method focuses on the symbolic sequence describing the topological change of the system which characterizes its bifurcation behavior. The concept of *block sequence* is first introduced. Based on the block sequence, the smoothness of the Poincaré map is described. Moreover, two main theorems are given to detect border collision and standard bifurcations. Finally, a specific example of the buck switching converter is presented to illustrate the application of the proposed symbolic analysis method. Using the proposed method, two-dimensional (2-D) bifurcation diagrams, which can assist engineers in identifying regions of preferred or undesired operations in the select parameter space, can be easily obtained.

**Index Terms**—Bifurcation, border collision, nonsmooth system, switching converter, symbolic analysis, symbolic sequence.

## I. INTRODUCTION

IN THE LAST decade, many nonlinear phenomena, such as bifurcations and chaos, have been identified in switching circuits and systems [1]–[3]. Detailed examinations of such phenomena have revealed that the underlying mechanisms can often be attributed to the switching operations that characterize this class of circuits and systems. For instance, switching power converters undergo topological changes cyclically in time. Although each involving circuit topology is linear and the dynamical behavior corresponding to each linear topology is easy to understand, the overall dynamics of switching power converters can be quite complicated. It has been shown previously that switching power converters can operate in a variety of regimes such as periodic operation, quasi-periodic operation and chaotic operation depending upon the choice of the parameters' values.

One important aspect of the research into nonlinear behavior of switching power converters is to investigate the different types of bifurcations and reveal their intrinsic mechanisms. In very general terms, there are two different types of bifurcations exhibited by switching power converters, namely *standard*

*bifurcation* and *border collision*. The former is characterized by a change of stability status, e.g., period-doubling, saddle-node, and Hopf bifurcations [4], whereas the latter is characterized by a change of operation as a result of a disruption of the operating topological sequence [3].

Specifically, it has been pointed out by Tse [3] that border collision occurs as a result of a “structural change” in the system when a parameter is varied. In the case of switching converters, this translates to a “change of topological sequence,” which is not observed when standard bifurcations occur. Consequently, this distinctive difference between a standard bifurcation and a border collision provides a possibility of investigating these bifurcations through the corresponding topological sequence that the system undergoes.

The purpose of this paper, unlike other previous studies, is to analyze the bifurcation in switching systems from the point of view of the operating topological sequences. The dynamics of the system can be examined from a symbolic sequence representing the topological sequence that the system assumes at any time and for any given set of parameters. This symbolic sequence naturally incorporates the information about the evolution of the circuit topology. From the symbolic sequence, the intrinsic mechanism of border collision can be exposed explicitly. To facilitate analysis, we define a new variable, *block sequence*, which can be used to distinguish border collision from other standard bifurcations. For readability and effectiveness of exposition, we will illustrate the application procedure using the voltage-mode controlled buck converter as an example. However, our method can be applied directly to other switching power converters.

## II. PRELIMINARIES

### A. Defining Border Collision

Much attention has been paid to the characterization of border collision in terms of how the qualitative behavior changes at border collision. However, definitions of border collision have been given mainly under specific contexts. In Di Bernardo *et al.* [5], it has been pointed out that for a piecewise-smooth dynamical system in continuous time, border collision occurs when the system trajectory becomes tangential to one of the phase space boundaries. In Nusse *et al.* [6]–[8] and Banerjee *et al.* [9], border collision is considered for piecewise-smooth one- and two-dimensional (1-, 2-D) maps. Specifically, Nusse *et al.* [6] defined border collision in terms of the difference of the sum of orbit

Manuscript received October 29, 2004; revised January 24, 2005. This work was supported by Hong Kong Research Grants Council under a competitive earmarked Research Grant PolyU 5241/03E. This paper was recommended by Associate Editor P. K. Rajan.

D. Dai and C. K. Tse are with the Department of Electronic and Information Engineering, Hong Kong Polytechnic University, Hong Kong (e-mail: encktse@polyu.edu.hk).

X. Ma is with the School of Electrical Engineering, Xi'an Jiaotong University, Xi'an, Shaanxi, China.

Digital Object Identifier 10.1109/TCSI.2005.852029

indices before and after the bifurcation. Moreover, Banerjee *et al.* [9] analyzed border collision and other bifurcations in 2-D piecewise-smooth maps in a 2-D parameter space. Since the dynamics of the system can be more conveniently studied in terms of its Poincaré map, a clear definition of border collision for discrete-time maps will be indispensable for further analysis. In the following, our discussion of border collision will be based upon discrete-time maps.

First, we observe that when border collision occurs in a piecewise-smooth map, there exists at least one point of the periodic orbit which lies exactly on the boundary that separates different appropriately defined smooth regions. Based on this basic feature, we may define border collision as follows.

*Definition 1:* Consider a piecewise-smooth map  $f(\mathbf{x}, \mu) : \mathbb{R}^{n+1} \rightarrow \mathbb{R}^n$ , where  $\mathbf{x} \in X \subseteq \mathbb{R}^n$  is the state and  $\mu \in I \subseteq \mathbb{R}$  is the parameter. Let  $\{X_i\}_{i=1,2,\dots,N}$  ( $N$  is a finite or infinite natural number) be a partition (or region) of the state space  $X$ , and  $X_i$  is smoothly dependent upon  $\mu$ . In each region  $X_i$ ,  $f \in C^1$  has a different smooth functional form. At the boundaries of these regions,  $f$  loses its smoothness, either being discontinuous or having discontinuous first derivative. If there exists  $\epsilon > 0$  such that in the neighborhood  $H(\mu_0) = \{\mu : |\mu - \mu_0| < \epsilon\}$  of  $\mu_0$ , the map has *different kinds of qualitative behavior* on the two sides of  $\mu_0$  and at least one point of the steady-state orbit lies on the boundaries when  $\mu = \mu_0$ , then **border collision** is said to occur at  $\mu = \mu_0$ .

In the above definition, the condition *different kinds of qualitative behavior*<sup>1</sup> deserves some special attention when it is applied to a piecewise-smooth map. Specifically, for a smooth map, periodic orbits, nonperiodic orbits, and periodic orbits with different periodicities are considered as being qualitatively different. Moreover, periodic orbits with the same periodicity are considered as the same kind of qualitative behavior. However, in a piecewise-smooth map, periodic orbits with the same periodicity can in fact be different kinds of qualitative behavior if the forms of the map leading to the corresponding periodic orbits are different.

Furthermore, it is worth noting that the above definition is consistent with those defined or implied in other publications. In brief we define border collision as the crossing of a fixed point or any point on a periodic orbit over boundaries of regions. In Di Bernardo *et al.* [5], as aforementioned, border collision has been observed in a continuous-time system when the trajectory becomes tangential to one of the phase space boundaries. Their subsequent analysis based upon local maps implies the location of the fixed points being on the borders that separate different regions of the local map. Moreover, in Nusse *et al.* [6]–[8], border collision has been studied directly on discrete maps. In particular, they defined border collision as the crossing of a fixed point over a border that separates two regions with different indices. They also showed that the fixed point is actually located on the border for the critical parameter value at border collision. Also, Banerjee *et al.* [9], [10] have basically the same interpretation, since their “borderlines” are essentially the boundaries of the regions mentioned in our aforesaid definition.

<sup>1</sup>Steady-state behavior is understood here. Thus, “different kinds of qualitative behavior” may include, inter alia, fixed points, limit cycles, quasi-periodic orbits, and chaotic orbits.

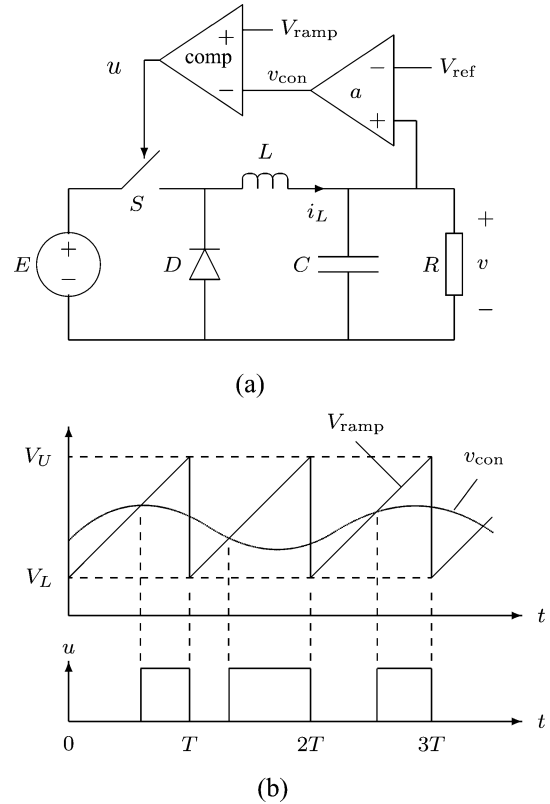


Fig. 1. Voltage-mode controlled buck converter. (a) Circuit. (b) Typical waveforms illustrating the operation.

### B. Theorem on Continuity of a Hyperbolic Fixed Point

The following theorem, addressing the continuity of a hyperbolic fixed point as some parameters are varied [11], is relevant to our subsequent study. However, for conciseness, we refer the readers to Robinson [11] for a detailed proof.

*Theorem 1:* Let  $f_\mu(\mathbf{x}) = f(\mathbf{x}, \mu)$  be a one-parameter family of differentiable maps with  $\mathbf{x} \in \mathbb{R}^n$  and  $\mu \in \mathbb{R}$ . Assume that  $f_\mu(\mathbf{x})$  is  $C^1$  as a function jointly of  $\mu$  and  $\mathbf{x}$ , and that  $f_{\mu_0}(\mathbf{x}_0) = \mathbf{x}_0$  and 1 is not an eigenvalue of  $D(f_{\mu_0})_{\mathbf{x}_0}$ . Then, there are (i) an open set  $U$  about  $\mathbf{x}_0$ , (ii) an interval  $W$  about  $\mu_0$ , and (iii) a  $C^1$  function  $\mathbf{p} : W \rightarrow U$  such that  $\mathbf{p}(\mu_0) = \mathbf{x}_0$  and  $f_\mu(\mathbf{p}(\mu)) = \mathbf{p}(\mu)$ . Moreover, for  $\mu \in W$ ,  $f_\mu$  has no fixed points in  $U$  other than  $\mathbf{p}(\mu)$ .

## III. GLIMPSE AT SWITCHING SYSTEMS: BUCK CONVERTER

We take a quick tour of a specific switching system, the objective being to expose some of the important features of switching systems. Specifically we consider the buck switching converter under a standard voltage-mode control, and examine its operation, describing vector field in continuous time, and Poincaré map in discrete time.

### A. Circuit Operation

The schematic diagram of the voltage-mode controlled buck converter is shown in Fig. 1(a). The operation of this buck converter can be briefly described as follows [3], [12]–[14]. The

output voltage error with respect to the reference voltage is amplified to give a control voltage  $v_{\text{con}}$  as

$$v_{\text{con}} = a(v - V_{\text{ref}}) \quad (1)$$

where  $v$  is the output voltage,  $a$  is the feedback amplifier gain, and  $V_{\text{ref}}$  is the reference voltage. Then, switch  $S$  is controlled by comparing the control voltage  $v_{\text{con}}$  with a ramp signal  $V_{\text{ramp}}$ . The ramp signal is given by

$$V_{\text{ramp}} = V_L + (V_U - V_L) \left( \frac{t}{T} \bmod 1 \right) \quad (2)$$

where  $V_L$  and  $V_U$  are the lower and upper thresholds of the ramp, respectively. The comparator output  $u$  gives the pulsewidth-modulated signal necessary for driving the switch, and is described by

$$u(v_{\text{con}}, t) = \begin{cases} 0, & \text{if } v_{\text{con}} > V_{\text{ramp}} \\ 1, & \text{if } v_{\text{con}} < V_{\text{ramp}}. \end{cases} \quad (3)$$

When  $u = 0$ , switch  $S$  is turned off, and when  $u = 1$ , switch  $S$  is turned on, as illustrated in Fig. 1(b). For simplicity, we consider continuous conduction mode (CCM), in which the inductor current never falls to zero. Thus, the system toggles between only two linear circuit topologies.

Two practical points are worth mentioning here. First, in practice, a more elaborate form of compensation network than a simple proportional control is often used in the feedback control. However, for the purpose of illustrating the effects of topological variation on the bifurcation behavior, it suffices to consider a simplified control circuit such as the one defined in (1), where only proportional feedback is included. Second, in most practical control schemes (with the exception of some low-cost implementations), a latch is included as part of the pulsewidth modulator to prevent multiple switchings in one clock period. Thus, topological variation is much richer in the absence of a latch, and our illustration of symbolic analysis can be more effective if the latch is excluded. Nonetheless, we should bear in mind that practical systems would be much limited in their topological variations (in other words, much simpler than the examples given here), but this should not affect the significance of our results.

### B. Vector Fields and Continuous-Time Description

The buck converter under study can be regarded as a second-order nonautonomous continuous-time dynamical system, which can be described by a state equation of the form

$$\dot{\mathbf{x}} = f(\mathbf{x}, t) \quad (4)$$

where  $\mathbf{x} = [x_1 \ x_2]^T = [v \ i]^T$  is the state vector (with superscript  $T$  denoting transposition) and  $f(\mathbf{x}, t)$  is the vector field. The system is nonautonomous because the vector field  $f(\mathbf{x}, t)$  is a function of time  $t$ . Moreover, the system is periodic with period  $T$  since  $f(\mathbf{x}, t) = f(\mathbf{x}, t + T)$  for any  $t$ . When the system assumes a specific circuit topology, the corresponding vector field is linear and continuous. However, the vector field of the system becomes discontinuous at the switching instants where

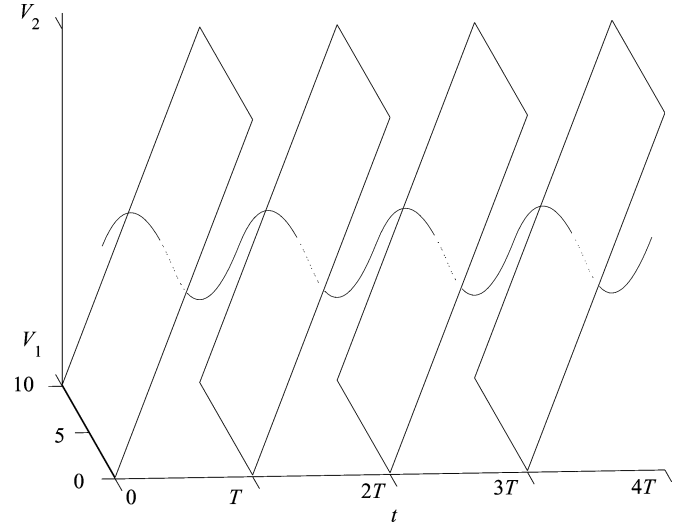


Fig. 2. Extended 3-D state space  $(x_1, x_2, t)$  showing zone  $\Omega_1$  and zone  $\Omega_2$  divided by the border  $B_s(\mathbf{x}, t)$  shown as the ramp planes. The region above these planes belongs to zone  $\Omega_1$ , and the region under these planes belongs to zone  $\Omega_2$ .

the circuit topology is changed.<sup>2</sup> Thus, the overall vector field is discontinuous and the system is a typical *piecewise-smooth dynamical system*.

Specifically, the vector field  $f(\mathbf{x}, t)$  can be defined as

$$f(\mathbf{x}, t) = \begin{pmatrix} -\frac{1}{RC} & \frac{1}{C} \\ -\frac{1}{L} & 0 \end{pmatrix} \mathbf{x} + \begin{pmatrix} 0 \\ \frac{E}{L} \end{pmatrix} u(\mathbf{x}, t). \quad (5)$$

The input term  $u(\mathbf{x}, t)$  in (5) is essentially equivalent to  $u(v_{\text{con}}, t)$  due to the affine relation between  $x_1$  and  $v_{\text{con}}$ , and can be written as

$$u(\mathbf{x}, t) = \begin{cases} 0, & \text{if } x_1 > v_{\text{ramp}} \\ 1, & \text{if } x_1 < v_{\text{ramp}}. \end{cases} \quad (6)$$

Here,  $v_{\text{ramp}}$  is obtained by an appropriate transformation of (2), which is given by

$$v_{\text{ramp}} = V_1 + (V_2 - V_1) \left( \frac{t}{T} \bmod 1 \right) \quad (7)$$

where  $V_1 = V_{\text{ref}} + V_L/a$  and  $V_2 = V_{\text{ref}} + V_U/a$ . The above equation effectively defines a switching border, which divides the state space into two parts, namely zone  $\Omega_1 = \{(\mathbf{x}, t) : x_1 > v_{\text{ramp}}\}$  and zone  $\Omega_2 = \{(\mathbf{x}, t) : x_1 < v_{\text{ramp}}\}$ . Thus, we may write the switching border  $B_s(\mathbf{x}, t)$  as

$$B_s(\mathbf{x}, t) = \{(\mathbf{x}, t) : x_1 = v_{\text{ramp}}\}. \quad (8)$$

As formulated previously by Ma, Kawakami, and Tse [13], the switching border for this system,  $B_s(\mathbf{x}, t)$ , is *periodically moving*, with period  $T$ , in the state space. Therefore, the buck converter under study can also be described as a switched dynamical system with a periodically moving border. To illustrate this moving border, we extend the 2-D state space  $(x_1, x_2)$  to the 3-D state space  $(x_1, x_2, t)$  by taking time  $t$  as an extra state, as shown in Fig. 2. For the sake of completeness (probably with

<sup>2</sup>At switching points, the state vector changes its orientation; the vector field, being the time-derivative of the state vector, is discontinuous.

no practical importance), we should also define  $u(\mathbf{x}, t)$  for the instant when  $x_1 = v_{\text{ramp}}$ . A consistent definition of  $u(\mathbf{x}, t)$ , for any  $(\mathbf{x}, t) \in B_s(\mathbf{x}, t)$ , can be precisely written as

$$u(\mathbf{x}, t)|_{(\mathbf{x}, t) \in B_s(\mathbf{x}, t)} = \begin{cases} u(\mathbf{x}(t - \epsilon), t - \epsilon), & \text{if } t \neq mT \\ 0, & \text{if } t = mT \\ & \text{and } \dot{x}_1(t^-) > \frac{V_2 - V_1}{T} \\ 1, & \text{if } t = mT \\ & \text{and } \dot{x}_1(t^-) \leq \frac{V_2 - V_1}{T}. \end{cases} \quad (9)$$

Here,  $m \in \mathbb{N}$ , and  $\epsilon > 0$  is sufficiently small.<sup>3</sup> Basically, what (9) gives is the precise state of the switch when  $x_1 = v_{\text{ramp}}$ , depending upon how the control signal  $x_1$  approaches the ramp signal  $v_{\text{ramp}}$ . Hence, (9) complements (6) in completing the definition of  $u(\mathbf{x}, t)$ , though is of little practical significance.

It is worth stressing that the arrival of the trajectory on the switching border does not necessarily imply switching. Switching takes place when the trajectory transversely crosses the border according to (6). Furthermore,  $v_{\text{ramp}}$  is discontinuous at  $t = mT$ , where switching occurs with  $u(\mathbf{x}, mT)$  going from 1 to 0 if  $x_1(mT) \in (V_1, V_2)$ .

### C. The Poincaré Map

As aforementioned, the vector field is discontinuous at switching instants and the buck converter under study is essentially a piecewise-smooth dynamical system. A classical technique for analyzing continuous-time dynamical systems is via a Poincaré map which describes the flow in terms of an iterative map [15]. For the time-periodic nonautonomous system with minimum period  $T$  described by (4), the Poincaré map is

$$P : \mathbb{R}^2 \rightarrow \mathbb{R}^2, \quad \mathbf{x} \mapsto P(\mathbf{x}) = \phi_{t_0+T}(\mathbf{x}, t_0) \quad (10)$$

where  $\phi_t(\mathbf{x}, t_0)$  is the solution to (4) with the initial condition  $\mathbf{x}(t_0) = \mathbf{x}$ , and  $t_0$  is conveniently taken as the start of any clock period.

The construction of  $P(\mathbf{x})$  involves stacking of the solutions of the individual vector fields given by (5) in the time interval  $[t_0, t_0 + T]$ . When  $u(\mathbf{x}, t)$  is equal to 0 or 1, the solution of the corresponding linear differential equation is readily found. Here, we denote the solutions by  $\varphi_0(\mathbf{x}_0, t)$  for  $u(\mathbf{x}, t) = 0$  (i.e., when the switch is off) and  $\varphi_1(\mathbf{x}_0, t)$  for  $u(\mathbf{x}, t) = 1$  (i.e., when the switch is on) with the initial condition  $\varphi_0(\mathbf{x}_0, 0) = \mathbf{x}_0$  and  $\varphi_1(\mathbf{x}_0, 0) = \mathbf{x}_0$ , respectively. Note that  $\varphi_0(\mathbf{x}_0, t), \varphi_1(\mathbf{x}_0, t) \in C^\infty$  with respect to time  $t$ . Thus,  $P(\mathbf{x})$  can be found in the form of a composition of  $\varphi_0$  and  $\varphi_1$ .

It should be noted that for all practical switching power converters consisting of incrementally passive components and no inductor-capacitor loops and/or cutsets, the solutions  $\varphi_0$  and  $\varphi_1$  are uniquely found. Hence, for a given *fixed topological sequence*, the Poincaré map  $P$  is homeomorphic.<sup>4</sup> This property is important in establishing the main results of this paper, as will be discussed in Section IV.

<sup>3</sup>As is customarily used in mathematics,  $\mathbb{N}$  is the natural numbers set.

<sup>4</sup>Homeomorphism literally means “similar correspondence” between two objects. Mathematically, a homeomorphic map is continuous, one-to-one, onto, and having a continuous inverse. Thus, adjective “global” or “local,” when applied to a homeomorphic map, specifies that the map is being homeomorphic over the entire state space or a region of the state space, respectively.

## IV. METHOD OF SYMBOLIC ANALYSIS OF BIFURCATION

### A. Symbolic Representation

For any given Poincaré map and an initial point, a *numerical orbit* can be generated by an iterative process, i.e.,

$$\mathbf{x}_0, \mathbf{x}_1, \mathbf{x}_2, \dots, \mathbf{x}_n, \dots \quad (11)$$

where  $\mathbf{x}_0$  is the initial point. Inspecting this orbit, the dynamics of the system can be studied.

Suppose we are only interested in knowing the region in which a point  $\mathbf{x}_i$  is located. We partition the state space into a finite or infinite number of smooth regions, each of which is denoted by a unique symbol. Here, we stress that we are now dealing with discrete state space, which will be implicitly assumed in our subsequent discussion. Then, from the numerical orbit, we can get a *symbolic sequence* or *symbolic orbit*

$$s_0, s_1, s_2, \dots, s_n, \dots \quad (12)$$

where  $s_i$  is the symbol representing the corresponding region to which  $\mathbf{x}_i$  belongs.

Clearly, the description using symbolic sequences is much cruder than that using the original numerical orbits [16], but it is much simpler and can still retain the essence of the dynamics. Since many different numerical orbits may correspond to the same symbolic sequence, classification of dynamical behavior may be more efficiently performed according to the type of symbolic sequence. Of course, the use of symbolic sequences in classification of dynamical behavior may suffer from a reduced level of differentiability (ability to distinguish different types of behavior), which has to be compensated by some additional identification procedures, as will be illustrated later in this paper.

When using symbolic sequences in the analysis of system dynamics, the way in which the state space is partitioned will play an important role. In fact, the essential dynamics can only be extracted from the symbolic sequence which has been generated with an appropriate state-space partitioning. For the buck converter studied here, it is intuitive to partition the state space according to the switching pattern that is being assumed in a switching period. For clarity of the subsequent discussion, we define two variables related to symbolic sequences.

**Definition 2:** A **switching block** is a sequence of switch states which is taken within one particular clock period (i.e., switching period in common engineering usage).<sup>5</sup>

**Definition 3:** A **block sequence** is a symbolic sequence of switching blocks that describes the way in which the block of switch states changes as time elapses.

From Definition 2, a sequence of switching states within a switching period is encapsulated into a switching block. Thus, the switching block is actually a symbolic series,  $\{c_n\}$ , where  $n = 1, \dots, N$ , with  $N - 1$  being the number of switchings that occur in this switching period (switchings that occur at the beginning and at the end of this switching period are not included). Here,  $c_n \in \{0, 1\}$ , where elements 0 and 1 represent the switch

<sup>5</sup>To avoid confusion, clock period is used in the above definition. In power electronics, however, “switching period” is also commonly used. Throughout the paper, we refer to “switching period” and “clock period” as the fixed period of time defined by an independent clock.

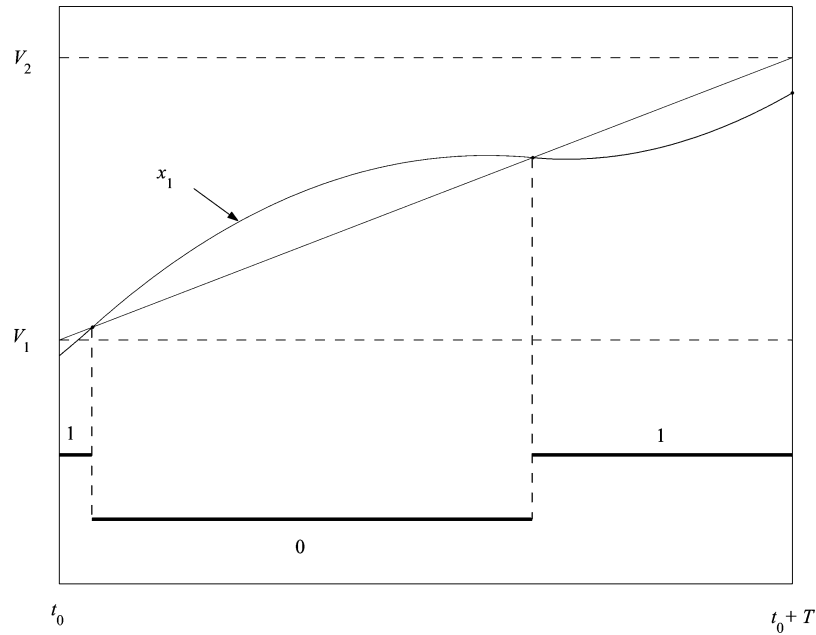


Fig. 3. Illustrative waveform of the switching block including symbol series 101. This block is denoted as block 6 according to the numbering rule (13).

states OFF and ON, respectively. Thus, for example, the following switching blocks are possible for any switching period:  $\{0\}$ ,  $\{1\}$ ,  $\{0,1\}$ ,  $\{1,0\}$ ,  $\{0,1,0\}$ ,  $\{1,0,1\}$ , etc. Suppose switching always bring along a change of the switch state from 0 to 1, or from 1 to 0. Then, a switching block will be uniquely determined if the total number of switchings and the initial switch state of this switching block are known. Hence, we may denote the switching block, which represents a symbol series  $(c_1 c_2 \cdots c_N)$ , according to the following (arbitrary) numbering rule

$$\text{block number} = \begin{cases} 2N - 1, & \text{if } c_1 = 0 \\ 2N, & \text{if } c_1 = 1 \end{cases} \quad (13)$$

where  $N - 1$  is the number of switchings in a period and  $c_1$  is the initial switch state of that period. Fig. 3 illustrates the correspondence between the control voltage waveform and the symbolic series of a specific switching block in the buck converter under study. According to the numbering rule (13), the block shown in Fig. 3 is block 6. Other blocks are illustrated in Fig. 4.

Now consider a point  $\mathbf{x}$  in the state space at time  $t_0$ . If the system assumes block  $b$  as its block sequence for the time interval  $[t_0, t_0 + T]$ , then we may write

$$b = \mathcal{L}(\mathbf{x}) \quad (14)$$

where  $\mathcal{L}$  is an operator which maps  $\mathbf{x} \in \mathbb{R}^2$  to a symbol  $b$  (i.e., a block number). Accordingly, the state space is divided into many regions. Each region is a set of points in the state space which are mapped to the same block, i.e.,  $\Pi_b = \{\mathbf{x} : \mathcal{L}(\mathbf{x}) = b\}$ , where  $\Pi_b$  is the region corresponding to block  $b$ . With this partitioning of the state space, the dynamics of the system can be described by a block sequence, such as the one given in (12). Furthermore, by examining the block sequence in conjunction

with other information,<sup>6</sup> bifurcation phenomena in the buck converter under study can be analyzed.

### B. Periodicity

Periodicity is an important aspect of the dynamical behavior of a system. However, inspecting the block sequence alone may not allow the periodicity of the system to be properly exposed. Now we need to distinguish two different types of periodicity. One is the traditional periodicity of the system's solution, precisely the *waveform periodicity*, which is denoted by  $p_w$ . For instance, a period- $n$  operation and a chaotic (quasi-periodic) operation correspond to  $p_w = n$  and  $p_w = \infty$ , respectively. The other is the *block sequence periodicity*, denoted by  $p_s$ . Obviously, for any periodic solution, its block sequence must be periodic. In particular, for a period- $n$  operation,  $p_s$  is a common divisor of  $n$ , which means  $p_s \leq n$ . Moreover, for an aperiodic solution, its block sequence may be aperiodic or periodic. Hence, *a periodic block sequence does not necessarily imply a periodic solution, but an aperiodic block sequence will imply an aperiodic solution*. To simplify the description of various kinds of block sequences, we use the following notations.

Let  $b_1, b_2, \dots, b_m$  be switching blocks. We denote by  $(b_1 b_2 \cdots b_m)_n$  a finite block sequence which repeats the block sequence  $(b_1 b_2 \cdots b_m)$   $n$  times. Moreover, a periodic block sequence is denoted as  $(b_1 b_2 \cdots b_m)_\infty$ , and an aperiodic block sequence as  $(\infty)$ .

### C. Some Properties of the Poincaré Map

As stated previously, the Poincaré map  $P(\mathbf{x})$  is constructed through stacking of a series of solutions. Thus, given  $\mathbf{x}$  at  $t_0$ , the form of  $P(\mathbf{x})$  is dependent upon the sequence of switch states

<sup>6</sup>As aforementioned, classification of dynamics based solely on the symbolic sequence may suffer reduced differentiability (ability to distinguish different types of behavior) to some extent. Supplementary information may be needed to reveal the dynamical behavior adequately. Such information will be discussed later.

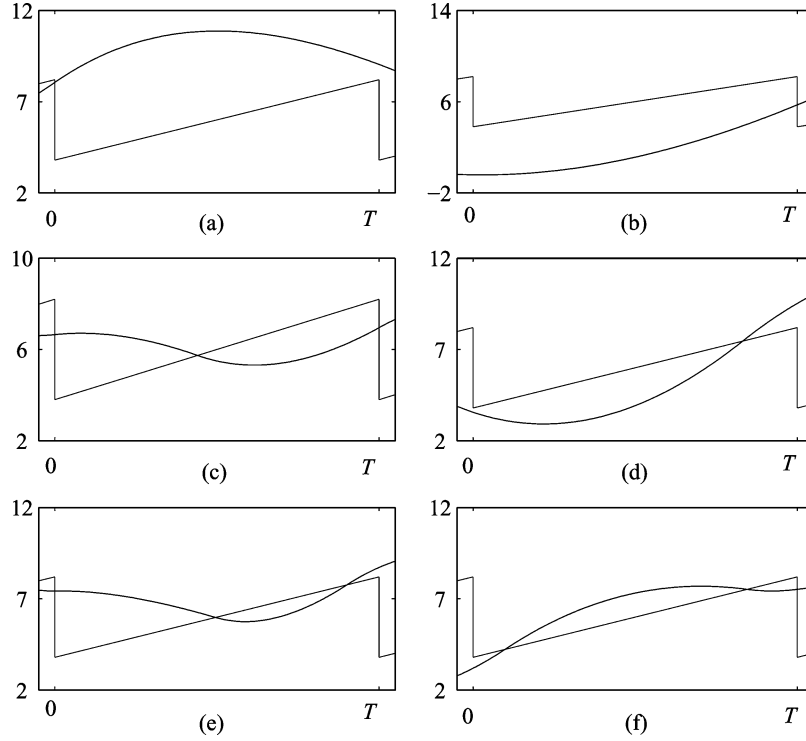


Fig. 4. Illustrative waveforms for different types of switching blocks. (a) Block **1** ( $N = 1, c_1 = 0$ ). (b) Block **2** ( $N = 1, c_1 = 1$ ). (c) Block **3** ( $N = 2, c_1 = 0$ ). (d) Block **4** ( $N = 2, c_1 = 1$ ). (e) Block **5** ( $N = 3, c_1 = 0$ ). (f) Block **6** ( $N = 3, c_1 = 1$ ).

from  $t_0$  to  $t_0 + T$ , i.e., the block to which  $\mathbf{x}$  belongs. For clarity, we summarize the procedure of deriving a specific  $P(\mathbf{x})$ , with  $\mathcal{L}(\mathbf{x}) = b$ , as follows.

Assume  $b = (c_1 c_2 \cdots c_N)$  and the switching instant between  $c_i$  and  $c_{i+1}$  is  $t_i$  for  $i = 1, \dots, N-1$ , with  $N > 1$ .<sup>7</sup> Then, the state at  $t_i$  can be obtained by the recurrent mapping

$$\mathbf{x}_i = \mathbf{x}(t_i) = \varphi_{c_i}(\mathbf{x}_{i-1}, t_i - t_{i-1}), \quad i = 1, \dots, N-1 \quad (15)$$

where  $\mathbf{x}_0 = \mathbf{x}(t_0) = \mathbf{x}$ . Thus

$$P(\mathbf{x}) = \varphi_{c_N}(\mathbf{x}_{N-1}, t_0 + T - t_{N-1}). \quad (16)$$

If we use the symbol  $c_i$  to denote the recurrent mapping described by (15), the Poincaré map can be simply written as

$$P(\mathbf{x}) = c_N \circ c_{N-1} \circ \cdots \circ c_2 \circ c_1(\mathbf{x}) \quad (17)$$

where operator  $\circ$  denotes composition.<sup>8</sup> This notation clearly emphasizes the relation between the Poincaré map and the switching block. Moreover, it can be concluded that the Poincaré maps for all  $\mathbf{x}$  in the region  $\Pi_b$  have the same form, which is denoted as  $P_b(\mathbf{x})$  here. Then, the Poincaré map is defined in the whole state space as

$$P(\mathbf{x}) = P_{b_m}(\mathbf{x}), \quad \text{for } \mathbf{x} \in \Pi_{b_m} \quad (18)$$

where  $m = 1, 2, \dots$ , and  $b_m$  represents a switching block. From (18), we know that  $P(\mathbf{x})$  is dependent upon  $\mathbf{x}$  and the symbolic series given in  $\mathcal{L}(\mathbf{x})$ . Thus, the Jacobian of  $P_b(\mathbf{x})$  will depend

<sup>7</sup>For  $N = 1$ ,  $P(\mathbf{x})$  is reduced to  $\varphi_{c_1}(\mathbf{x}, T)$ .

<sup>8</sup>Essentially, (17), and hence (18), should include all switching instants  $t_i$  and corresponding states  $\mathbf{x}_i$  ( $i = 1, \dots, N-1$ ). For simplicity, these intermediate variables are not shown in the equation since they are implicitly dependent upon  $\mathbf{x}$ .

on both  $b$  and  $\mathbf{x}$  since  $P_b(\mathbf{x})$  is essentially a composition of  $N$   $C^\infty$  functions.

In Olivar *et al.* [17], the structure of the regions corresponding to different numbers of switchings in a switching period in the state space was studied. The regions considered in Olivar *et al.* [17] are actually equivalent to the regions defined here. In particular, it has been shown [17] that the whole state space is divided into a doubly infinite number of regions by the line  $r_l$  and the curve  $s_l$ , and each region is a connected set, where  $r_l = \{\mathbf{x} : x_1 = V_1\}$  and  $s_l = P^{-1}(r_u)$  with  $r_u = \{\mathbf{x} : x_1 = V_2\}$ . The curve  $s_l$  is a piecewise-smooth double spiral which intersects the line  $r_l$  with a bi-infinite sequence of points. It is easy to show that the boundary of any two regions is a subset of  $B = r_l \cup s_l$ . The basic structure of the state space is illustrated in Fig. 5, which has been numerically computed. Furthermore, it can be shown that the Poincaré map  $P(\mathbf{x})$  for any switching converter is continuous and homeomorphic in each of the regions,<sup>9</sup> but is piecewise-smooth (differentiable). Also, in each region excluding its boundaries,  $P(\mathbf{x})$  is smooth, which means that  $P_{b_m}(\mathbf{x})$  in (18) is smooth if  $\mathbf{x}$  is an inner point of  $\Pi_{b_m}$ .

The following proposition, a version of which was proved in Olivar *et al.* [17] for the buck converter, will be useful in our subsequent analysis. This proposition is applicable to all switching converters whose Poincaré maps are homeomorphic in every region of the state space partitioned in the above fashion, i.e.,

<sup>9</sup>As mentioned before, for power converters consisting of incrementally passive components and no inductor-capacitor loops and/or cutsets, a unique solution is guaranteed for any given topological sequence. Hence, the Poincaré map is homeomorphic within any region where the topological sequence is fixed. Local homeomorphism of  $P$  is thus guaranteed for all switching converters. For the buck converter under voltage-mode control,  $P$  is globally homeomorphic [17].

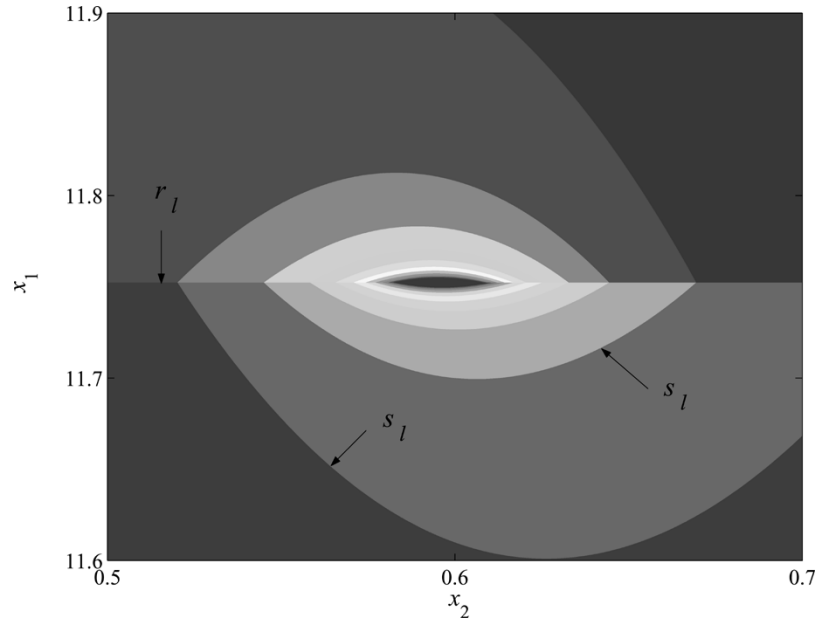


Fig. 5. Partitions of the state space for the voltage-mode controlled buck converter with  $L = 0.02$  mH,  $C = 47$   $\mu$ F,  $R = 22$   $\Omega$ ,  $T = 400$   $\mu$ s,  $a = 8.4$ ,  $V_{\text{ref}} = 11.3$  V,  $V_L = 3.8$  V,  $V_U = 8.2$  V (i.e.,  $V_1 = 11.752$  V,  $V_2 = 12.276$  V) and  $E = 28$  V. It is clearly observed that different regions are separated by the double spiral  $s_i$  together with the line  $r_i$ .

within every region of fixed topological sequence. See Olivar *et al.* [17] for a proof.

*Proposition 1:*  $P$  is smooth (differentiable) at  $\mathbf{x}_0$  if, and only if, there exists some neighborhood  $H(\mathbf{x}_0)$  of  $\mathbf{x}_0$  such that  $P$  is locally homeomorphic at  $\mathbf{x}_0$  and  $\mathcal{L}(\mathbf{x}) = \mathcal{L}(\mathbf{x}_0)$  for all  $\mathbf{x} \in H(\mathbf{x}_0)$ .

#### D. Some Properties of $P^n$

We will study some qualitative properties of  $P^n$ , where superscript  $n$  denotes the  $n$ th iteration. For example,  $P^0(\mathbf{x}) = \mathbf{x}$ ,  $P^2(\mathbf{x}) = P(P(\mathbf{x}))$ , etc.

Suppose  $(\mathbf{x}_1, \mathbf{x}_2, \dots, \mathbf{x}_n)$  is a period- $n$  orbit. Then, we have

$$\begin{aligned} \mathbf{x}_{i+1} &= P(\mathbf{x}_i), & \text{for } i = 1, 2, \dots, n-1 \\ \mathbf{x}_1 &= P(\mathbf{x}_n). \end{aligned} \quad (19)$$

Thus,  $\mathbf{x}_i$  ( $i = 1, 2, \dots, n$ ) can be considered as the fixed point of the map  $P^n$ .

Now, given an initial point  $\mathbf{x}$ , by iterating it  $n - 1$  times, a series of  $n$  points can be obtained as  $(P^0(\mathbf{x}), P^1(\mathbf{x}), P^2(\mathbf{x}), \dots, P^{n-1}(\mathbf{x}))$ . From Definition 3, this series corresponds to a block sequence, say  $(b_1 b_2 \dots b_n)$ , with  $b_i = \mathcal{L}(P^{i-1}(\mathbf{x}))$  for  $i = 1, 2, \dots, n$ . Denoting this block sequence by  $\mathbf{L}$ , we may define the symbolic representation of any point  $\mathbf{x}$  in the state space under map  $P^n$  as

$$\mathbf{L} = \mathcal{L}_n(\mathbf{x}) \quad (20)$$

where  $\mathcal{L}_n$  maps  $\mathbf{x} \in \mathbb{R}^2$  to a block sequence  $(b_1 b_2 \dots b_n)$ .

Intuitively speaking, since  $P$  is piecewise-smooth, so is its composition  $P^n$ . The following propositions clarify this property. These propositions will be used in proving our main results, to be presented in the next subsection. The proofs are given in the Appendix.

*Proposition 2:*  $P^n$  is smooth (differentiable) at  $\mathbf{x}_0$  if, and only if, there exists some neighborhood  $H(\mathbf{x}_0)$  of  $\mathbf{x}_0$  such that  $P$  is locally homeomorphic in  $H(\mathbf{x}_0)$  and  $\mathcal{L}_n(\mathbf{x}) = \mathcal{L}_n(\mathbf{x}_0)$  for all  $\mathbf{x} \in H(\mathbf{x}_0)$ .

*Proposition 3:* Let  $\mathbf{x}_i = P^i(\mathbf{x}_0)$  for  $i = 0, 1, \dots, n-1$ . Suppose  $P$  is locally homeomorphic in some neighborhood  $H(\mathbf{x}_0)$  of  $\mathbf{x}_0$ . Then,  $P^n$  is not smooth at  $\mathbf{x}_0$  if, and only if, there exists at least one  $\mathbf{x}_i$  such that  $\mathbf{x}_i \in B$ . (Here,  $B$  is the union of the boundaries of all regions as defined previously.)

It should be noted that, as mentioned before, the Poincaré map  $P$  for all switching converters is homeomorphic in each region of the state space corresponding to a fixed topological sequence. Moreover, this local homeomorphic property of  $P$  is meaningful only when we consider practical parameter ranges. Thus, throughout the paper, it is understood that the local homeomorphic property, when required, applies only to practical parameter ranges. In other words, we do not care about impractical conditions such as the case where the output voltage is bigger than the input voltage for a buck converter, which is practically absurd.

At this point, several important consequences arisen from the above propositions, which are pivotal to understanding the structure of the state-space partitioning of the different regions described earlier, are worth noting.

- 1) Proposition 2 provides a direct relation between the block sequence and the smoothness of the map  $P^n$ . Moreover, Proposition 3 gives the sufficient and necessary condition for the map  $P^n$  to lose its smoothness. Thus, the elementary structure of the state space in relation to the block sequence can be qualitatively established as follows. The whole state space is divided into an infinite number of regions. In each region,  $P^n$  is smooth and  $\mathcal{L}_n(\mathbf{x})$  remains identical for any point  $\mathbf{x}$  in this region. The smoothness

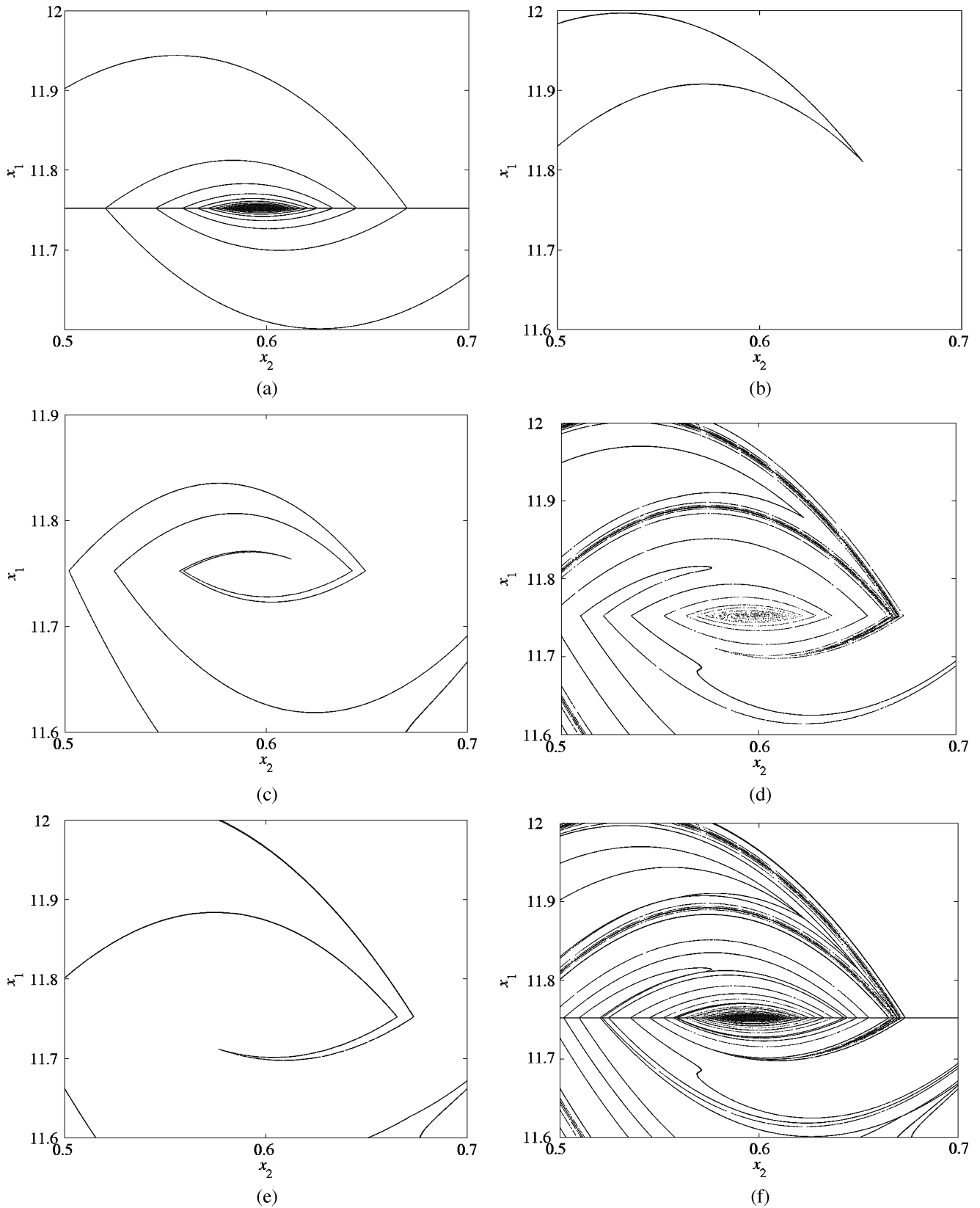


Fig. 6. Illustration of the boundary of  $P^5$ . The parameters used here are the same as those in Fig. 5. (a)  $B^0$ . (b)  $B^{-1}$ . (c)  $B^{-2}$ . (d)  $B^{-3}$ . (e)  $B^{-4}$ . (f)  $B(P^5)$ .

will be lost on the boundaries which separate different regions. In other words,  $P^n$  is also piecewise-smooth and has a similar structure in the state space as that of  $P$  in a topological sense.

2) The local homeomorphic property of  $P$  is necessary for the proofs of Propositions 2 and 3. See the Appendix. For switching converters,  $P$  is homeomorphic in each region defined according to the previously described state-

space partitioning scheme. (Basically, under this partitioning scheme, each region corresponds to one topological sequence.) Moreover, for the buck converter under voltage-mode control, it has been shown that  $P$  is in fact globally homeomorphic [17], which may facilitate finding of the specific boundary for  $P^n$ . Let  $B^i = P^{-1}(B^{i+1})$  for  $i = -1, -2, \dots, -n+1$ . Now, let  $B^0 = B$ . Since  $B^0$  is a union of a curve and a line,  $B^i$  will also be a union of two curves under the homeomorphic transformation of  $P^{-1}$ . Thus, from Proposition 3, the boundary of the map  $P^n$  is  $B(P^n) = \bigcup_{i=0, -1, \dots, -n+1} B^i$ , which forms the borders of the partitioned state space of  $P^n$ . As an illustrative example, Fig. 6 shows  $B^0, B^{-1}, B^{-2}, B^{-3}, B^{-4}$  and their union  $B(P^5)$ . These boundary curves are obtained numerically, all parameters being the same as those used in Fig. 5.

- 3) Suppose  $(\mathbf{x}_1, \mathbf{x}_2, \dots, \mathbf{x}_n)$  is a period- $n$  orbit of  $P$ . Then, these  $n$  points are the fixed points of  $P^n$ . If there exists one  $\mathbf{x}_i \in B^0$ , then  $\mathbf{x}_i \in B(P^n)$  for all  $i = 1, 2, \dots, n$ . On the other hand, if there exists one  $\mathbf{x}_i \in B(P^n)$ , then  $\mathbf{x}_i \in B(P^n)$  for all  $i = 1, 2, \dots, n$  and there is at least one  $\mathbf{x}_i$  such that  $\mathbf{x}_i \in B^0$

#### E. Detecting Border Collision and Standard Bifurcations: Main Theorems

We present our main results, summarized in two theorems, for detecting border collision and standard bifurcations using symbolic analysis. All symbols used (e.g.,  $P^i, B^i$ , etc.) are consistent with those defined in Section IV-D.

**Theorem 2:** Consider a switching system with parameter  $\mu \in \mathbb{R}$ . Suppose its Poincaré map is locally homeomorphic in each state-space region corresponding to a given topological sequence. Suppose that there exists some interval  $H(\mu_0)$  of  $\mu_0$ , and that the system is periodic for either  $\mu < \mu_0$  or  $\mu > \mu_0$  or both. In the parameter interval  $H(\mu_0)$ , the block sequences in the steady state are  $\mathbf{L}_1$  and  $\mathbf{L}_2$  for  $\mu < \mu_0$  and  $\mu > \mu_0$ , respectively. Then, border collision occurs at  $\mu = \mu_0$  if  $\mathbf{L}_1 \neq \mathbf{L}_2$ .<sup>10</sup>

*Proof:* Without loss of generality, assume that the system has a period- $n$  orbit  $(\mathbf{x}_1(\mu), \mathbf{x}_2(\mu), \dots, \mathbf{x}_n(\mu))$  when  $\mu \in (\mu_1, \mu_0] \subset H(\mu_0)$ . This implies that  $P^n$  is smooth and has a stable fixed point  $\mathbf{x}_1(\mu)$  for  $\mu \in (\mu_1, \mu_0)$ . Then,  $P^n$  must be nonsmooth at  $\mathbf{x}_1(\mu_0)$  when  $\mu = \mu_0$ . Otherwise, if  $P^n$  is smooth at  $\mathbf{x}_1(\mu_0)$  when  $\mu = \mu_0$ , from Theorem 1 there exists  $\varepsilon > 0$  such that  $P^n$  has a stable fixed point  $\mathbf{x}_1(\mu)$  which is smoothly dependent on  $\mu$  for  $\mu_0 - \varepsilon < \mu < \mu_0 + \varepsilon$ . Thus,  $\mathcal{L}_n(\mathbf{x}_1(\mu))$  remains identical for  $\mu_0 - \varepsilon < \mu < \mu_0 + \varepsilon$ , which means  $\mathbf{L}_1 = \mathbf{L}_2$ , contradicting the assumption that  $\mathbf{L}_1 \neq \mathbf{L}_2$ . Therefore,  $P^n$  must be nonsmooth at  $\mathbf{x}_1(\mu_0)$  when  $\mu = \mu_0$ . Then, from Proposition 3, there exists at least one  $\mathbf{x}_i(\mu_0)$  ( $i = 1, 2, \dots, n$ ) such that  $\mathbf{x}_i(\mu_0) \in B^0$  when  $\mu = \mu_0$ . Since  $\mathbf{L}_1 \neq \mathbf{L}_2$ , the system has different dynamical behaviors on the two sides of  $\mu_0$ . Thus, from Definition 1, border collision occurs at  $\mu = \mu_0$ . *Q.E.D.*

<sup>10</sup>Strictly speaking, it is possible that the steady-state solutions are aperiodic on the two sides of  $\mu_0$  and  $\mathbf{L}_1 \neq \mathbf{L}_2$ . We exclude this case from this theorem, as comparison of two block sequences corresponding to aperiodic solutions is impractical.

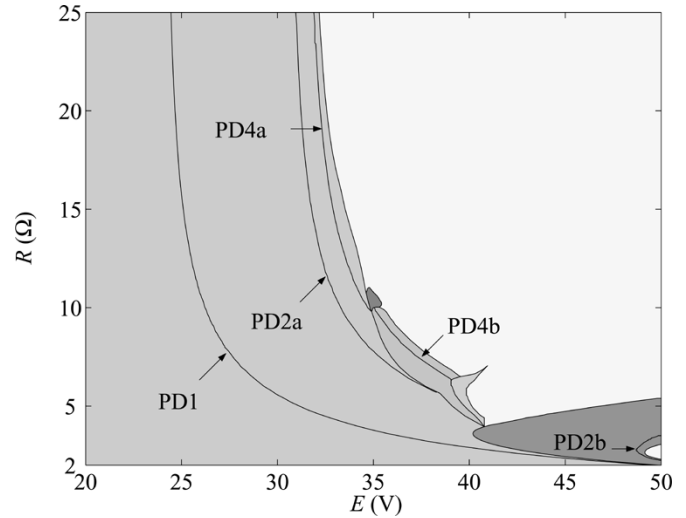


Fig. 7. Bifurcation diagram in the parameter plane  $\{(R, E) : 2 \leq R \leq 25; 20 \leq E \leq 50\}$  from symbolic analysis. Light blue:  $(3)_{\infty}$ ; magenta:  $(35)_{\infty}$ ; red:  $(13\ 333\ 333)_{\infty}$ ; green:  $(1333)_{\infty}$ ; cyan:  $(13\ 331\ 335)_{\infty}$ ; yellow: the rest including chaotic and periodic operating regions. Boundary curves separating regions of different colors locate the occurrence of border collision. Within a specific region, bifurcation boundary curves corresponding to PD1, PD2a, PD2b, PD4a, and PD4b are also plotted. These curves locate the standard period doublings.

**Theorem 3:** Consider a switching system with parameter  $\mu \in \mathbb{R}$ . Suppose its Poincaré map is locally homeomorphic in each state-space region corresponding to a given topological sequence. Suppose there exists some interval  $H(\mu_0)$  of  $\mu_0$ . In this parameter interval  $H(\mu_0)$ , the block sequences of the steady state are  $\mathbf{L}_1$  and  $\mathbf{L}_2$  for  $\mu < \mu_0$  and  $\mu > \mu_0$ , respectively. Moreover, the waveform periodicities of the steady state are  $p_{w1}$  and  $p_{w2}$  for  $\mu < \mu_0$  and  $\mu > \mu_0$ , respectively. Then, standard bifurcation occurs at  $\mu = \mu_0$  if  $\mathbf{L}_1 = \mathbf{L}_2$  and  $p_{w1} \neq p_{w2}$ .

*Proof:* Since  $p_{w1} \neq p_{w2}$ , some kind of bifurcation must occur at  $\mu = \mu_0$ . From Proposition 2, the condition  $\mathbf{L}_1 = \mathbf{L}_2$  implies that  $P^n$  is smooth at any orbit point of the steady state when  $\mu = \mu_0$ . Thus, no orbit point of the steady state belongs to  $B^0$  when  $\mu = \mu_0$ . Otherwise, from Proposition 2,  $P^n$  is not smooth at such an orbit point when  $\mu = \mu_0$ . This contradicts the result implied from the condition  $\mathbf{L}_1 = \mathbf{L}_2$ . Therefore, border collision cannot occur when  $\mu = \mu_0$ , and the bifurcation occurred at  $\mu = \mu_0$  must be a standard bifurcation. *Q.E.D.*

Theorems 2 and 3 provide a symbolic method for detecting both border collision and standard bifurcations. As will be demonstrated in the next section, this method is very simple and fast because no heavy computation is required for the entire process of detection.

#### V. SYMBOLIC ANALYSIS OF BUCK CONVERTER UNDER VOLTAGE-MODE CONTROL: AN EXAMPLE

We apply the proposed symbolic analysis to a specific voltage-mode controlled buck converter. By numerical computations, a 2-D bifurcation diagram covering both border collision and standard period-doubling bifurcation can be plotted efficiently in the parameter plane.

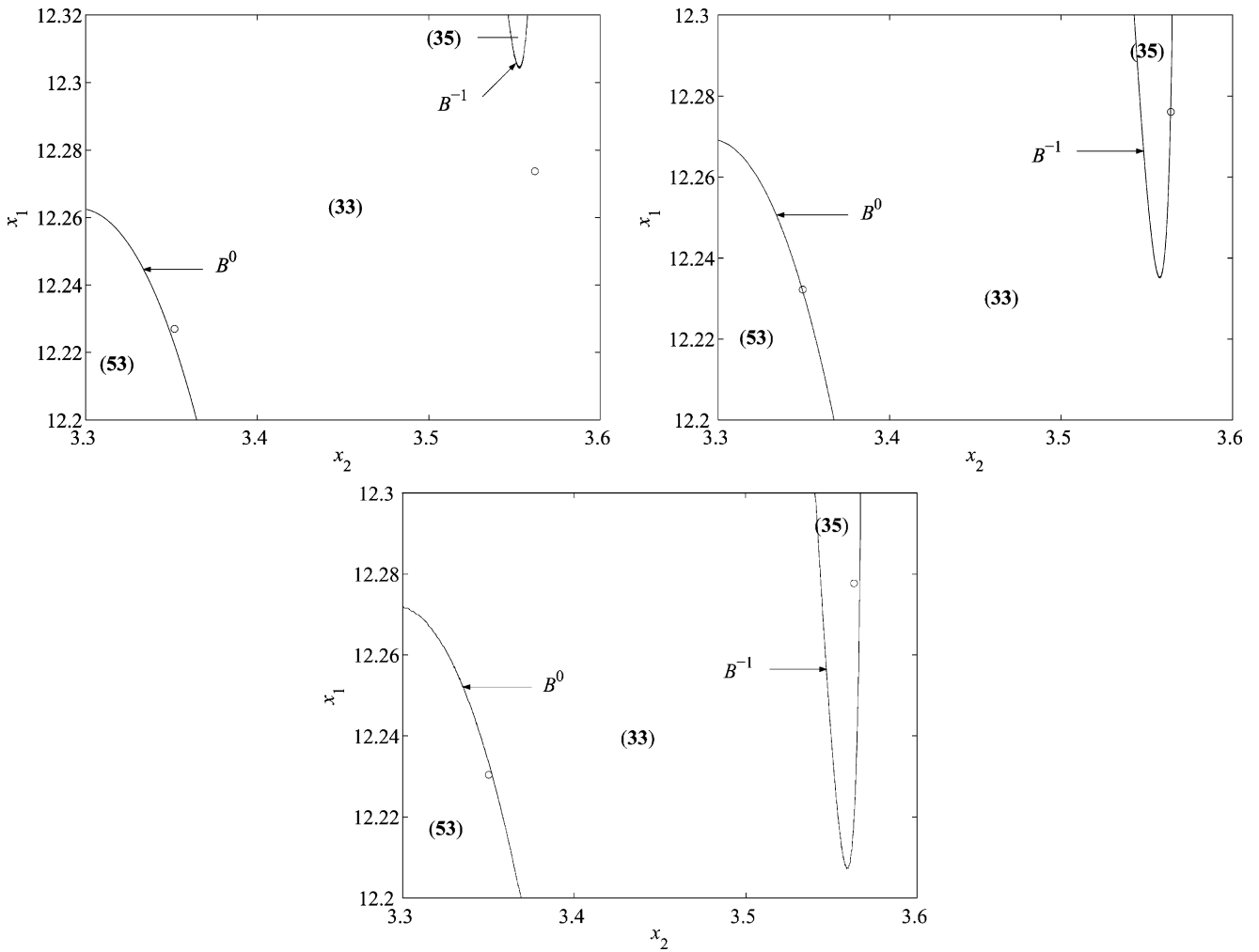


Fig. 8. Phase portraits and the boundaries  $B(P^2)$  when border collision occurs. The load resistor  $R$  is fixed to  $3.6 \Omega$  and the input voltage  $E$  is varied as follows. (a)  $E = 40.0 \text{ V}$ . (b)  $E = 40.18 \text{ V}$ . (c)  $E = 40.25 \text{ V}$ . The state space shown in this figure is partitioned into three regions corresponding to block sequence (53), (33), and (35), respectively. The boundary of these regions is  $B(P^2)$  which consists of  $B_0$  and  $B^{-1}$ .

To guarantee operation in CCM, the parameters are chosen as follows:

$$L = 20 \text{ mH}, \quad C = 47 \mu\text{F}, \quad T = 400 \mu\text{s}, \quad a = 8.4$$

$$V_{\text{ref}} = 11.3 \text{ V}, \quad V_L = 3.8 \text{ V} \text{ and } V_U = 8.2 \text{ V}.$$

The load resistor  $R$  and the input voltage  $E$  are varied simultaneously and taken as bifurcation parameters.

Applying the symbolic analysis, we obtain the 2-D bifurcation diagram shown in Fig. 7. In this diagram, the parameter plane is divided into different regions according to their block sequences, as explained earlier. For simplicity, only some main regions are illustrated and shown in different colors. From Theorem 2, we know that border collision occurs on the boundaries that separates regions of different colors. Further, each region of the same color may also be divided into several subregions by some boundary curves, across which the waveform periodicities  $p_w$  are changed. Specifically,  $p_w$  are doubled when the parameters move across these curves from left to right. Thus, these curves correspond to *period-doubling bifurcations*, and are denoted by  $\text{PD}ni$ , where  $n$  is the lower  $p_w$  associated with the period doubling and  $i$  is an index for the same  $n$ . Since the

color does not change when the parameters move across a specific curve, a standard period-doubling bifurcation takes place on that curve according to Theorem 3. For example, border collision takes place with block sequence  $(\mathbf{3})_\infty$  being transmuted to  $(\mathbf{1333})_\infty$  when the parameters move from the grey region to the green region. Moreover, a standard period-doubling bifurcation occurs with the same block sequence  $(\mathbf{3})_\infty$  when the parameters move across the curve  $\text{PD1}$  from left to right.

Furthermore, we show in Fig. 8 some phase portraits for the purpose of illustrating the characteristic change of the block sequence when border collision occurs. Here, the state space is partitioned into three regions by the boundaries  $B(P^2)$  which correspond to block sequences (53), (33), and (35). When  $R$  is fixed at  $3.6 \Omega$  and  $E$  is around  $40.18 \text{ V}$ , the system has a period-two orbit and each orbit point is a fixed point of  $P^2$ . Fig. 8 clearly shows the variation of the block sequence from  $(\mathbf{3})_\infty$  to  $(\mathbf{53})_\infty$  (or  $(\mathbf{35})_\infty$ ) when  $E$  moves across  $E = 40.18 \text{ V}$ . Also, the orbit points are located on the boundary  $B(P^2)$  when  $E = 40.18 \text{ V}$ . Therefore, border collision takes places at  $E = 40.18 \text{ V}$  with block sequence  $(\mathbf{3})_\infty$  being transmuted to  $(\mathbf{35})_\infty$  with the period unchanged.

## VI. CONCLUSION

In this paper, the bifurcation behavior of switching systems has been studied from the symbolic dynamical viewpoint. Unlike conventional methods, our method focuses on the characteristic change of the symbolic sequence when the system undergoes a specific bifurcation. For this purpose, the concept of block sequence is introduced to describe the symbolic sequence of the system. Then, it is shown that the loss of smoothness of the Poincaré map and its composition is relevant to the change of the corresponding block sequence. Two theorems are derived for detecting border collision and standard bifurcations, and a specific example is also given to illustrate the method. Although the symbolic method proposed here is only applied to a voltage-mode controlled buck converter, the basic methodology of using symbolic sequences for bifurcation analysis is applicable to other switching circuits or piecewise-smooth dynamical systems.

## APPENDIX

### Proof of Proposition 2

*Proof of the “only if” part:* Assume  $\mathcal{L}_n(\mathbf{x}) = \mathcal{L}_n(\mathbf{x}_0)$  for all  $\mathbf{x} \in H(\mathbf{x}_0)$ , where  $H(\mathbf{x}_0)$  is some neighborhood of  $\mathbf{x}_0$ . Let  $\mathcal{L}_n(\mathbf{x}_0) = \mathbf{L}$ , where  $\mathbf{L}$  represents the block sequence  $(b_1 b_2 \cdots b_n)$ . Since  $\mathbf{L}(\mathbf{x}) = b_1$  for all  $\mathbf{x} \in H(\mathbf{x}_0)$ ,  $P$  is smooth at  $\mathbf{x}_0$  from Proposition 1. Then, since  $P$  is locally homeomorphic in  $H(\mathbf{x}_0)$ ,  $P$  maps  $H(\mathbf{x}_0)$  to  $H_1(\mathbf{x}_1)$ , where  $\mathbf{x}_1 = P(\mathbf{x}_0)$  and  $H_1(\mathbf{x}_1)$  is the corresponding neighborhood of  $\mathbf{x}_1$ . Since  $\mathbf{L}(\mathbf{x}) = b_2$  for all  $\mathbf{x} \in H_1(\mathbf{x}_1)$ ,  $P$  is also smooth at  $\mathbf{x}_1$  from Proposition 1. Thus, by the chain rule of differentiation,  $P^2 = P \circ P$  is smooth at  $\mathbf{x}_0$ . Repeating the above procedure, we conclude that  $P^n$  is smooth at  $\mathbf{x}_0$ .

*Proof of the “if” part:* Assume that there does not exist a neighborhood  $H(\mathbf{x}_0)$  of  $\mathbf{x}_0$  such that  $\mathcal{L}_n(\mathbf{x}) = \mathcal{L}_n(\mathbf{x}_0)$  for all  $\mathbf{x} \in H(\mathbf{x}_0)$ . This means that for any neighborhood  $H(\mathbf{x}_0)$  of  $\mathbf{x}_0$ , there exists  $\mathbf{x} \in H(\mathbf{x}_0)$  such that  $\mathcal{L}_n(\mathbf{x}) \neq \mathcal{L}_n(\mathbf{x}_0)$ . Then, two sequences  $\{x_m\}_{m \in \mathbb{N}}$  and  $\{H_m(\mathbf{x}_0)\}_{m \in \mathbb{N}}$  can be found such that  $\mathbf{x}_m \in H_m(\mathbf{x}_0)$  and  $\mathcal{L}_n(\mathbf{x}_m) \neq \mathcal{L}_n(\mathbf{x}_0)$  with  $\lim_{m \rightarrow \infty} \mathbf{x}_m = \mathbf{x}_0$ . Now, denote the Jacobian of  $P$  at point  $\mathbf{x}$  as  $JP(\mathbf{x})$ . Then, the Jacobian of  $P^n$  at  $\mathbf{x}$  is

$$JP^n(\mathbf{x}) = JP(P^{n-1}(\mathbf{x})) \cdot JP(P^{n-2}(\mathbf{x})) \cdots JP(P(\mathbf{x})) \cdot JP(\mathbf{x}). \quad (21)$$

Let  $\mathbf{x}_{i,j} = P^j(\mathbf{x}_i)$  for  $i = 0$  or  $i \in \mathbb{N}$  and  $j = 0, 1, \dots, n-1$ . Then,

$$JP^n(\mathbf{x}_0) = JP(\mathbf{x}_{0,n-1}) \cdot JP(\mathbf{x}_{0,n-2}) \cdots JP(\mathbf{x}_{0,1}) \cdot JP(\mathbf{x}_{0,0}) \quad (22)$$

and

$$JP^n(\mathbf{x}_m) = JP(\mathbf{x}_{m,n-1}) \cdot JP(\mathbf{x}_{m,n-2}) \cdots JP(\mathbf{x}_{m,1}) \cdot JP(\mathbf{x}_{m,0}), \quad \text{for } m \in \mathbb{N}. \quad (23)$$

Since  $\mathcal{L}_n(\mathbf{x}_m) \neq \mathcal{L}_n(\mathbf{x}_0)$ ,  $\lim_{m \rightarrow \infty} JP^n(\mathbf{x}_m) \neq JP^n(\mathbf{x}_0)$ . Thus, we have found a sequence  $\{x_m\}_{m \in \mathbb{N}}$  such that  $\lim_{m \rightarrow \infty} x_m = x_0$ . However,  $\lim_{m \rightarrow \infty} JP^n(\mathbf{x}_m) \neq$

$JP^n(\mathbf{x}_0)$ . This means that  $P^n$  is not smooth at  $\mathbf{x}_0$ . Obviously, the result derived from the assumption is contradictory to the condition that  $P^n$  is smooth at  $\mathbf{x}_0$ . Therefore, the assumption does not hold.

### Proof of Proposition 3

*Proof of the “only if” part:* Assume that there exists one  $\mathbf{x}_i$  such that  $\mathbf{x}_i \in B$ . Then, for any neighborhood  $H(\mathbf{x}_i)$  of  $\mathbf{x}_i$ , there must exist  $\mathbf{x} \in H(\mathbf{x}_i)$  such that  $\mathcal{L}(\mathbf{x}) \neq \mathcal{L}(\mathbf{x}_i)$  since  $\mathbf{x}_i \in B$ . Thus, we cannot find a neighborhood  $H(\mathbf{x}_0)$  of  $\mathbf{x}_0$  such that  $\mathcal{L}_n(\mathbf{x}) = \mathcal{L}_n(\mathbf{x}_0)$  for all  $\mathbf{x} \in H(\mathbf{x}_0)$ . From Proposition 2,  $P^n$  is not smooth at  $\mathbf{x}_0$ .

*Proof of the “if” part:* Assume  $\mathbf{x}_i \notin B$  for any  $\mathbf{x}_i$ . Then we can find a neighborhood  $H(\mathbf{x}_0)$  of  $\mathbf{x}_0$  such that the successive  $i$  ( $i = 1, 2, \dots, n-1$ ) times mapping of  $H(\mathbf{x}_0)$  together with  $H(\mathbf{x}_0)$  itself does not include any point which belongs to  $B$ . This means  $\mathcal{L}_n(\mathbf{x}) = \mathcal{L}_n(\mathbf{x}_0)$  for any  $\mathbf{x} \in H(\mathbf{x}_0)$ . Thus, from Proposition 2, it implies that  $P^n$  is smooth at  $\mathbf{x}_0$ . This result is contradictory to the condition that  $P^n$  is not smooth at  $\mathbf{x}_0$ . Therefore, the assumption does not hold.

## REFERENCES

- [1] S. Banerjee and G. Verghese, Eds., *Nonlinear Phenomena in Power Electronics*. New York: IEEE Press, 2000.
- [2] C. K. Tse and M. di Bernardo, “Complex behavior of switching power converters,” *Proc. IEEE*, vol. 90, no. 5, pp. 768–781, May 2002.
- [3] C. K. Tse, *Complex Behavior of Switching Power Converters*. Boca Raton, FL: CRC, 2003.
- [4] J. M. T. Thompson and H. B. Stewart, *Nonlinear Dynamics and Chaos*. Chichester, U.K.: Wiley, 2000.
- [5] M. di Bernardo, M. I. Feigin, and S. J. Hogan, “Local analysis of C-bifurcations in n-dimensional piecewise-smooth dynamical system,” *Chaos, Solitons Fractals*, vol. 10, no. 11, pp. 1881–1908, 1999.
- [6] H. E. Nusse and J. A. Yorke, “Border-collision bifurcations including ‘period two to period three’ for piecewise-smooth systems,” *Physica D*, vol. 57, no. 1, pp. 39–57, Jun. 1992.
- [7] H. E. Nusse, E. Ott, and J. A. Yorke, “Border-collision bifurcations: an explanation for observed bifurcation phenomena,” *Phys. Rev. E*, vol. 49, no. 2, pp. 1073–1078, Feb. 1994.
- [8] H. E. Nusse and J. A. Yorke, “Border-collision bifurcations for piecewise-smooth one-dimensional maps,” *Int. J. Bifur. Chaos*, vol. 5, no. 1, pp. 189–207, Jan. 1995.
- [9] S. Banerjee, P. Ranjan, and C. Grebogi, “Bifurcations in two-dimensional piecewise-smooth maps—Theory and applications in switching circuits,” *IEEE Trans. Circuits Syst. I, Fundam. Theory Appl.*, vol. 47, no. 5, pp. 633–643, May 2000.
- [10] S. Banerjee, E. Ott, J. A. Yorke, and G. H. Yuan, “Anomalous bifurcations in dc-dc converters: borderline collisions in piecewise-smooth maps,” in *IEEE Power Electron. Specialists Conf.*, 1997, pp. 1337–1344.
- [11] C. Robinson, *Dynamical Systems: Stability, Symbolic Dynamics, and Chaos*. Boca Raton, FL: CRC, 1999.
- [12] E. Fossas and G. Olivar, “Study of chaos in the buck converter,” *IEEE Trans. Circuits Syst. I, Fundam. Theory Appl.*, vol. 43, no. 1, pp. 13–25, Jan. 1996.
- [13] Y. Ma, H. Kawakami, and C. K. Tse, “Analysis of bifurcation in switched dynamical systems with periodically moving borders,” *IEEE Trans. Circuits Syst. I, Fundam. Theory Appl.*, vol. 51, no. 6, pp. 1184–1193, Jun. 2004.
- [14] M. di Bernardo and F. Vasca, “Discrete-time maps for the analysis of bifurcations and chaos in dc/dc converters,” *IEEE Trans. Circuits Syst. I, Fundam. Theory Appl.*, vol. 47, no. 2, pp. 130–143, Feb. 2000.
- [15] T. S. Parker and L. O. Chua, *Practical Numerical Algorithms for Chaotic Systems*. New York: Springer-Verlag, 1989.
- [16] B.-L. Hao and W. M. Zheng, *Applied Symbolic Dynamics and Chaos*, Singapore: World Scientific, 1998.
- [17] G. Olivar, E. Fossas, and C. Batlle, “Bifurcation and chaos in converters: discontinuous vector fields and singular Poincaré maps,” *Nonlinearity*, vol. 13, no. 4, pp. 1095–1121, Jul. 2000.



**Dong Dai** (M'05) was born in Huaiyin, Jiangsu Province, China, in 1976. He received the B.E. and Ph.D. degrees, both in electrical engineering, from Xi'an Jiaotong University, China, in 1998 and 2003, respectively.

Since 2003, he has been a Research Associate with Hong Kong Polytechnic University, Hong Kong, China. His research interests include chaos control and synchronization, nonlinear phenomena in electrical engineering, and numerical analysis of electromagnetic field.

Dr. Dai was the recipient of many scholarships and awards during his undergraduate and graduate studies, including "Star of Science and Technology" awarded by Xi'an Jiaotong University, China. His Ph.D. dissertation also won the Distinguished Thesis Award from Xi'an Jiaotong University in 2003.



**Chi K. Tse** (M'90-SM'97) received the B.Eng. (Hons) degree with first class honors in electrical engineering and the Ph.D. degree from the University of Melbourne, Australia, in 1987 and 1991, respectively.

He is presently a Chair Professor with Hong Kong Polytechnic University, Hong Kong, and his research interests include chaotic dynamics and power electronics. He is the author of *Linear Circuit Analysis* (London, U.K.: Addison-Wesley, 1998) and *Complex Behavior of Switching Power Converters*

(Boca Raton: CRC, 2003), coauthor of *Chaos-Based Digital Communication Systems* (Heidelberg, Germany: Springer-Verlag, 2003) and a *Signal Reconstruction With Applications to Chaos-Based Communications* (Beijing, China: Tsinghua University Press, 2005), and coholder of a U.S. patent.

Dr. Tse was awarded the L. R. East Prize by the Institution of Engineers, Australia, in 1987. He won the IEEE TRANSACTIONS ON POWER ELECTRONICS Prize Paper Award for 2001 and the *International Journal of Circuit Theory and Applications* Best Paper Award for 2003. From 2005 to 2006, he serves as an IEEE Distinguished Lecturer. While with Hong Kong Polytechnic University, he received twice the President's Award for Achievement in Research, the Faculty's Best Researcher Award, the Research Grant Achievement Award and a few other teaching awards. He served as an Associate Editor for the IEEE TRANSACTIONS ON CIRCUITS AND SYSTEMS PART I—FUNDAMENTAL THEORY AND APPLICATIONS, from 1999 to 2001, and since 1999, has been an Associate Editor for the IEEE TRANSACTIONS ON POWER ELECTRONICS. He currently also serves as an Associate Editor for the *International Journal of Systems Science*, a Guest Associate Editor of the *IEICE Transactions on Fundamentals of Electronics, Communications and Computers*, and a Guest Editor of *Circuits, Systems and Signal Processing*. Since 2002, he has been a Guest Professor of Southwest China Normal University, Chongqing, China.



**Xikui Ma** was born in Shaanxi, China, in 1958. He received the B.E. and M.Sc. degrees, both in electrical engineering, from Xi'an Jiaotong University, China, in 1982 and 1985, respectively.

In 1985, he joined the Xi'an Jiaotong University as a Lecturer, and since 1992, he has been a Professor with the same university. His research interests include electromagnetic field theory and its applications, numerical methods, modeling of magnetic components, chaotic dynamics and its applications in power electronics, and applications of digital control

in power electronics. He has been actively involved in more than 15 research and development projects. He is the author of *Electromagnetic Field Theory and Its Applications* (Xi'an: Xi'an Jiaotong University Press, 2000) and has published more than 130 technical papers.

Prof. Ma received the Best Teacher Award from Xi'an Jiaotong University in 1999.